Mechanisms for the Expulsion of Propene from Ionized Propyl Phenyl Ethers in the Gas Phase

John C. Traeger[†] and Thomas Hellman Morton*,[‡]

Contribution from the School of Chemistry, LaTrobe University, Bundoora, Victoria, Australia, and Department of Chemistry, University of California, Riverside, California 92521-0403

Received March 8, 1996[⊗]

Abstract: Unimolecular dissociation of ionized, deuterium-substituted propyl phenyl ethers has been investigated by means of photoionization mass spectrometry as a technique for insuring that different isotopomers can be compared at the same internal energy. Elimination of neutral propene is the only ionic fragmentation detected in the energy domain studied but is found to take place via competing pathways. The contrast between measured fragment ion ratios from parent ions having internal energies 0.8 eV above the dissociation barriers, HOPh[•+]:DOPh[•+] = 1.23 for PhOCH$_2$CH$_2$CD$_3$ (**1c**) *versus* HOPh[•+]:DOPh[•+] ≥ 1.38 for PhOCH(CD$_3$)CH$_3$ (**4b**), demonstrates that **4b**[•+] is not an obligatory intermediate in the dissociation of **1c**[•+]. Examination of ten other deuterated analogues of *n*-propyl phenyl ether permits an assignment of branching ratios. There are two ways to interpret the data using first-order kinetics: a phenomenological analysis (which considers the contributions from different chain positions) and a mechanistic analysis (which considers competition among four pathways). These two analyses lead to different conclusions, and the mechanistic analysis is to be preferred. For **1c** the molecular ion decomposes predominantly (>90%) via a [CD$_3$CHCH$_3$$^+$ PhO•] ion−neutral complex, with an additional 7% passing through complexes that randomize hydrogen within the propyl cation. Only 1% of ionized **1c** fragments via site-specific β-transfer from the propyl side chain. Slightly more than 1% decomposes via site-specific γ-transfer, which can be ascribed to intervention of ion−neutral complexes containing unrearranged, corner-protonated cyclopropanes. Correction for these alternative pathways leads to the conclusion that the primary isotope effect for the Brønsted acid-base reaction between isopropyl cation and phenoxy radical within ion−neutral complexes has a value $k_H/k_D = 1.21$. Proportions of the various pathways for ionized *n*-propyl phenyl ethers depend on the isotopic substitution pattern. Nearly one-sixth of PhOCD$_2$CH$_2$CD$_3$ (**1d**) molecular ions decompose via site-specific β-transfer or γ-transfer (in a ratio of 1:1.1). The increased competition in this d_5 analogue accounts for the reported conformational dependence of its supersonic jet/REMPI mass spectrum.

Despite its ostensible simplicity, heterolysis of the C−X bond in ions of the form CH$_3$CH$_2$CH$_2$X$^+$ has proven to be quite a complicated reaction. Because the nascent CH$_3$CH$_2$CH$_2$$^+$ structure does not correspond to a stable geometry,[1] the propyl group isomerizes in concert with departure of the leaving group X. Isotopic labeling studies in solution reveal that 1,2-hydride transfer to form isopropyl cation (the global minimum on the C$_3$H$_7$$^+$ potential energy surface) is not always the initial rearrangement.[2] The role of solvent in guiding the reaction is not clear. Hence it warrants exploration in the gas phase. This paper examines C−O bond heterolysis of ionized *n*-propyl phenyl ether, *n*PrOPh[•+] to form ion−neutral complexes. Photoionization mass spectrometry of *n*PrOPh and 11 deuterated analogues provides a data set from which we measure branching ratios and infer an unanticipated mechanism operating in competition with those previously described.

Product ratios are analyzed in terms of first-order kinetics. This type of analysis can be rigorously applied in two limiting cases: either where reactant molecules are monoenergetic (isolated and all having the same internal energy), or where they are thermalized and in contact with an infinite heat bath.[3] While first-order kinetics has been used in the past to interpret

data from intermediate regimes, those quantitative conclusions must be viewed as approximate, at best. The present study uses first differential photoionization efficiency curves to extract data corresponding to the monoenergetic limit. The results for the *n*-propyl phenyl ethers are compared with those for deuterated isopropyl phenyl ethers.

Background

Thirty years ago MacLeod and Djerassi described the complete lack of regioselectivity in the expulsion of butene from ionized *n*-butyl phenyl ether in the gas phase.[4] By separately labeling each carbon of the alkyl chain with deuterium, they showed that the mass spectrum exhibits a mixture of HOPh[•+] (*m/z* 94) and DOPh[•+] (*m/z* 95), regardless of which position is deuterated. A decade later Benoit and Harrison reported the same phenomenon in the decomposition of ionized *n*-propyl phenyl ether (*n*PrOPh, **1**).[5] Their analysis of the mass spectra of PhOCD$_2$CH$_2$CH$_3$ (**1a**), PhOCH$_2$CD$_2$CH$_3$ (**1b**), and PhOCH$_2$CH$_2$CD$_3$ (**1c**) suggested that the selection from among the α-, β-, and γ-positions in eq 1 is nearly statistical.

$$\alpha \quad \beta \quad \gamma$$
$$\text{PhOCH}_2\text{CH}_2\text{CH}_3 \xrightarrow{-e^-} n\text{PrOPh}^{+\bullet} \xrightarrow{-\text{C}_3\text{H}_6} \text{HOPh}^{+\bullet} \quad (1)$$
$$\mathbf{1}$$

In that same year (1976) two other pertinent papers appeared. Collection and analysis of the neutral fragments expelled from

---

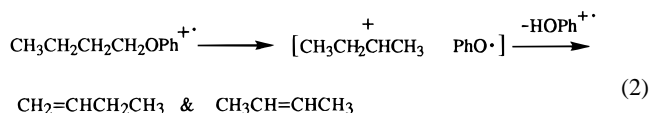[†] LaTrobe University.

[‡] University of California, Riverside.

[⊗] Abstract published in *Advance ACS Abstracts,* September 15, 1996.

(1) Koch, W.; Liu, B.; Schleyer, P. v. R. *J. Am. Chem. Soc.* **1989,** *111,* 3479−3480.
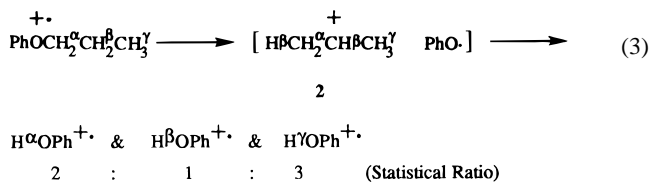
(2) (a) Lee, C. C.; Cessna, A. J.; Ko, E. C. F.; Vassie, S. *J. Am. Chem. Soc.* **1973**, *95,* 5688−5692. (b) Vogel, P. *Carbocation Chemistry*; Elsevier: Amsterdam, 1985; pp 330−335.

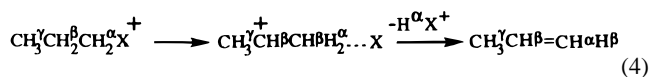(3) Klots, C. E. In *Unimolecular and Bimolecular Ion-Molecule Reactions*; Wiley: 1994; pp 311−335.

(4) MacLeod, J. K.; Djerassi, C. *J. Am. Chem. Soc.* **1966**, *88,* 1840−1841.

(5) Benoit, F. M.; Harrison, A. G. *Org. Mass Spectrom.* **1976**, *11,* 599−608.

ionized *n*-butyl phenyl ether (the first experiment of its kind)[6] showed that 1- and 2-butenes constitute >95% of the expelled C_4H_8, and the distribution of isotopic label in the neutral products corroborated the mass spectrometric results of

$$CH_3CH_2CH_2CH_2OPh^{+\bullet} \longrightarrow [CH_3CH_2\overset{+}{C}HCH_3 \quad PhO\bullet] \overset{-HOPh^{+\bullet}}{\longrightarrow}$$

$$CH_2=CHCH_2CH_3 \quad \& \quad CH_3CH=CHCH_3 \tag{2}$$

MacLeod and Djerassi. With regard to *n*PrOPh, a Field Ionization Kinetics study demonstrated that the lack of regioselectivity in the expulsion of C_3H_6 is manifested at the very shortest time scales (10^{-11} s) on which HOPh$^{\bullet+}$ fragment ions could be detected.[7]

$$PhOC\overset{\alpha}{H_2}C\overset{\beta}{H_2}C\overset{\gamma}{H_3}^{+\bullet} \longrightarrow [H\beta C\overset{\alpha}{H_2}CH\beta C\overset{\gamma}{H_3} \quad PhO\bullet] \longrightarrow \tag{3}$$

2

$$H^{\alpha}OPh^{+\bullet} \quad \& \quad H^{\beta}OPh^{+\bullet} \quad \& \quad H^{\gamma}OPh^{+\bullet}$$

$$\quad 2 \quad : \quad 1 \quad : \quad 3 \quad \text{(Statistical Ratio)}$$

In 1980 one of us proposed the intervention of ion–neutral complexes to account for all of these results,[8] as represented for ionized *n*-butyl phenyl ether in eq 2. This type of mechanism accounted not only for eq 2 but also for alkene expulsion from a variety of other ionized primary alkyl phenyl ethers.[9] The C_4H_8 isomer distribution in eq 2 corresponds to a comparatively cold cation (even though the ionized precursor was formed by 70 eV electron impact), with less methylcyclopropane formation than is observed from *n*-butyldiazonium ions in solution.[10] Extending this interpretation to eq 1 presupposed that all of the hydrogens randomize in the $C_3H_7^+$ cation within a $[C_3H_7^+ \ PhO^\bullet]$ ion–neutral complex, **2**.

$$C\overset{\gamma}{H_3}C\overset{\beta}{H_2}C\overset{\alpha}{H_2}X^+ \longrightarrow C\overset{\gamma}{H_3}\overset{+}{C}H\beta CH\beta H\overset{\alpha}{H_2}\cdots X \overset{-H^{\alpha}X^+}{\longrightarrow} CH_3CH\beta=CH\alpha H\beta \tag{4}$$

That hypothesis was further explored in a two-color Resonance Enhanced Multiphoton Ionization (REMPI) study of $PhOCD_2CH_2CD_3$ (**1d**) and **1b**.[11] After a naive correction for isotope effect, the ratio of α- and γ-hydrogen transfer to β-hydrogen transfer was found to be $R = 2.5$, just as would be predicted by the hydrogen scrambling mechanism. By contrast, the value of the ratio in the electron impact Mass Resolved Ion Kinetic Energy Spectrum (MIKES) was measured to be $R = 4.3$. This latter result can easily be incorporated into the mechanistic hypothesis: at the lower internal energies of ions studied by MIKES, the $C_3H_7^+$ cations within the ion–neutral complexes undergo slow transposition of hydrogen, reacting (for the most part) as though the complex contains an isopropyl cation that undergoes no further rearrangement. This latter mechanism is represented in eq 3 and predicts a statistical ratio of $R = 5$. (The same ratio would obtain if the ionized *n*-propyl ether simply isomerized to the ionized isopropyl ether.)
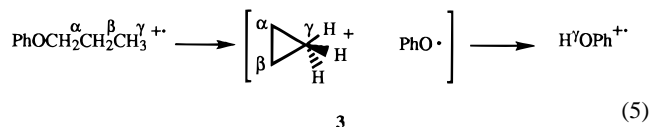
We contrast the mechanism in eq 3 with pure vicinal elimination or 1,5-hydrogen shift from the propyl chain to the

ring, either of which would proceed via β-hydrogen transfer and would have given a ratio of $R = 0$. Thus we list three mechanistic options for propene expulsion (in order of increasing value of the $\alpha,\gamma{:}\beta$ ratio): (*i*) β-elimination or 1,5-hydrogen shift ($R = 0$); (*ii*) hydrogen randomization ($R = 2.5$); (*iii*) *n*-Pr → *i*Pr isomerization or intervention of an $[iPr^+ \ PhO^\bullet]$ ion–neutral complex with no additional hydrogen transposition ($R = 5$).

We must add to this list the option of predominant α-transfer, as reported by Veith and Gross in propene expulsion from metastable $nPr_2N=CH_2^+$.[12] This can be interpreted (based on ab initio calculations on the stable complexes between *n*-propyl cation and ammonia[13]) as stemming from a hydrogen-bonded complex between the newly-formed methyl group and the departing base, which eq 4 depicts. This mechanism thus constitutes a fourth option: (*iv*) α-elimination ($R = \infty$).

It would seem from this panoply of mechanisms that any experimental result could be fit by some combination of options *i*–*iv*. For example, one-color REMPI of indvidual conformers of **1b** and **1d** in supersonic jets gives HOPh$^{\bullet+}$:DOPh$^{\bullet+}$ ratios that correspond to values of R within experimental error of 2.5.[14] While parsimony suggests option *ii* as a likely interpretation, the jet/REMPI experiments show that the HOPh$^{\bullet+}$:DOPh$^{\bullet+}$ ratio from **1d** varies significantly (ANOVA: $F = 14.00$, df = 37) among the three conformational isomers whose (0,0)-bands were examined. Such variation is hard to comprehend if only a single pathway operates but is readily understood if two (or more) pathways are in competition. In recent studies of $PhSCH_2CH_2CH_3$ and of substituted propyl aryl ethers Nibbering and co-workers[15] propose just such a composite mechanism, embracing options *i*–*iii*.

The barrier to eq 1 has recently been experimentally determined to be 1.47 eV.[16] For mass spectrometers with time scales on the order of 1–10 μs kinetic shifts >0.5 eV are expected. In such an apparatus one ought not to observe the onset of fragmentation until the parent ions have internal energies $\geq$2 eV. Consequently a conventional mass spectrometric experiment looks at the products of ion–neutral complexes that contain $\geq$0.7 eV, more than twice the energy difference between isopropyl cation (the most stable $C_3H_7^+$ isomer) and corner-protonated cyclopropane.[1]

$$PhOC\overset{\alpha}{H_2}C\overset{\beta}{H_2}C\overset{\gamma}{H_3}^{+\bullet} \longrightarrow \left[\text{(corner-protonated cyclopropane)} \quad PhO\bullet \right] \longrightarrow H^{\gamma}OPh^{+\bullet} \tag{5}$$

3

The experimental results below provide evidence for contribution from a previously unexamined pathway, exemplified by eq 5. This pathway corresponds to exclusive γ-hydrogen transfer and represents a fifth option: (*v*) γ-Elimination via intervention of an ion–neutral complex containing an unrearranged corner-protonated cyclopropane or via a γ-distonic intermediate ($R = \infty$).

Experimental Section

Compounds **1b** and **1d** were synthesized as previously reported.[11] Deuterium was introduced into the other compounds using LiAlD$_4$. Compound **1a** was prepared from propionic acid; **1c**, **1g**, and **1k** from

(6) Burns, F. B.; Morton, T. H. *J. Am. Chem. Soc.* **1976**, *98*, 7308–7313.

(7) Borchers, F.; Levsen, K.; Beckey, H. D. *Int. J. Mass Spectrom. Ion Phys.* **1976**, *21*, 125–132.

(8) Morton, T. H. *J. Am. Chem. Soc.* **1980**, *102*, 1596–1602.

(9) McAdoo, D. J.; Morton, T. H. *Acc. Chem. Res.* **1993**, *26*, 295–302.

(10) Friedman, L.; Bayless, J. H. *J. Am. Chem. Soc.* **1969**, *91*, 1790–1794.

(11) Chronister, E. L.; Morton, T. H. *J. Am. Chem. Soc.* **1990**, *112*, 133–139.

(12) Veith, H. J.; Gross, J. H. *Org. Mass Spectrom.* **1991**, *26*, 1097–1108.

(13) Audier, H. E.; Morton, T. H. *Org. Mass Spectrom.* **1993**, *28*, 1218–1224.

(14) Song, K.; van Eijk, A.; Shaler, T. A.; Morton, T. H. *J. Am. Chem. Soc.* **1994**, *116*, 4455–4460.

(15) (a) van Amsterdam, M. W.; Ingemann, S.; Nibbering, N. M. M. *J. Mass Spectrom.* **1995**, *30*, 43–51. (b) Matimba, H. E.; Ingemann, S.; Nibbering, N. M. M. *J. Mass Spectrom.* **1996**, *31*, 609–622.

(16) Weddle, G.; Dunbar, R. C.; Song, K.; Morton, T. H. *J. Am. Chem. Soc.* **1995**, *117*, 2573–2580.
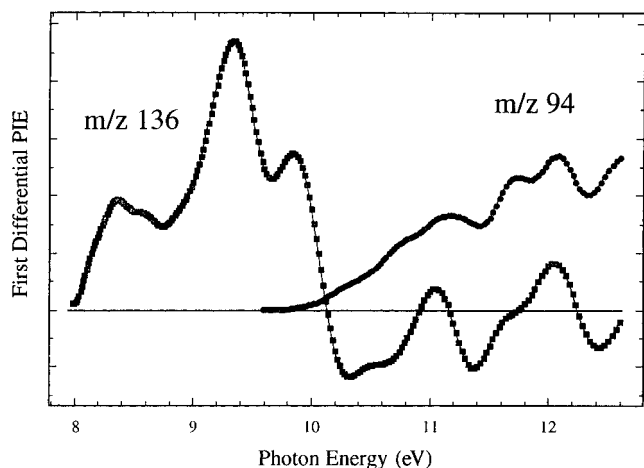
Figure 1. First differential photoionization efficiency (PIE) curves for the molecular ion (*m/z* 136) and the sole fragment ion (*m/z* 94) from undeuterated *n*-propyl phenyl ether (**1**).

3-phenoxypropionic acid; **1e** from propionic-2,2-d_2 acid (Aldrich); **1f** and **1j** from 3-phenoxy-1,2-epoxypropane (Aldrich); **1h** from phenoxyacetone; **1i** from propionaldehyde; and **4a** and **4b** from 2-phenoxypropionic acid. Chemical purity ≥98% (except for traces of solvent) was assessed by GLC/MS analysis. Most compounds were purified by two successive distillations at atmospheric pressure (bp 180−185° for the *n*-propyl phenyl ethers; bp 170−175° for the isopropyl phenyl ethers). As previously reported, **1d** contains about 8% of d_4 isotopomers,[11] and **1f** is estimated to contain 3% **1b** and 5% **1j**. From mass spectrometry the remaining deuterated compounds were gauged to be ≥99 atom% D. While the measured HOPh•+:DOPh•+ ratios from **1d** and **1f** might be as much as 10% too high (owing to incomplete deuteration), experimental *m/z* 94:*m/z* 95 ratios were corrected only for 6.6% natural ^{13}C abundance and not for incomplete deuteration.

The apparatus for measuring photoionization efficiency (PIE) curves has been described in detail elsewhere.[17] Briefly, a microcomputer-controlled photoionization mass spectrometer makes use of the hydrogen pseudocontinuum and a Seya−Namioka monochromator equipped with a holographically ruled diffraction grating.[18] The resolution of the monochromator was fixed at 1.35 Å, and the absolute energy scale was calibrated with atomic emission lines to an accuracy of better than 0.003 eV. All experiments were performed at ambient temperature (297 K) with sample pressures of 10^{-3} Pa in the ion-source region. Flight time between the ionization source and the mass selector is estimated to be on the order of 5 μs. Experimental adiabatic 0 K ionization energies (IEs) correspond to the first observed vibrational progression peak in the molecular ion first differential PIE curve. All differential PIE curves were obtained from the experimental data using a 15-point Fourier transform filter for smoothing with the program HORIZON (Star Blue Software, Inc.) before simple first derivatives were taken.[19] Phenomenological and mechanistic models were fitted to the experimental HOPh•+:DOPh•+ ratios using the MINSQ nonlinear least-squares program in the SCIENTIST package (Micromath, Inc.). Branching ratios for the mechanistic model were determined at the energy (10.35 eV) corresponding to the first minimum in the molecular ion intensity above the onset of fragmentation in the first differential PIE curve (*cf.* Figure 1). Ab initio UHF geometries were optimized with the 6-31G** basis set using GAUSSIAN94 (Gaussian, Inc.) on the Cray C90 at the San Diego Supercomputing Center and SPARTAN (Wavefunction, Inc.) software. Potential energy minima were confirmed by means of analytical frequency calculations.

(17) (a) Traeger, J. C.; McLoughlin, R. G. *J. Am. Chem. Soc.* **1981**, *103*, 3647−3652. (b) Traeger, J. C.; McLoughlin, R. G.; Nicholson, A. J. C. *J. Am. Chem. Soc.* **1982**, *104*, 5318−5322. (c) Traeger, J. C. *Int. J. Mass Spectrom. Ion Processes* **1984**, *58*, 259−271.

(18) Traeger, J. C. *Rapid Commun. Mass Spectrom.* **1996**, *10*, 119−122.

(19) Traeger, J. C.; Hudson, C. E.; McAdoo, D. J. *J. Am. Soc. Mass Spectrom.* **1996**, *7*, 73−81.

Experimental Results

Previous studies have investigated compounds **1a**−**d** to assess positional selectivity. From the experimental HOPh•+:DOPh•+ ratios proportions of α-, β-, and γ-transfer (expressed in terms of the mole fractions corresponding to undeuterated **1**: X_α, X_β, and X_γ) can be estimated. Since no previous study has looked at more than four different deuterated analogues at one time, a uniform isotope effect has had to be assumed in order to extract phenomenological partial relative rate factors from the data (*i.e.*, to assign contributions from each position of the carbon chain). Such a dissection also presumes that ion decay obeys first-order kinetics, which does not adequately describe the general case for unimolecular decay of a collection of reactive ions having a distribution of internal energies.[20,21]

We have enthusiastically made use of these two approximations in the past. In the present study, however, a larger number of deuterated analogues permits determination of separate isotope effects for positions α, β, and γ. Analysis of the HOPh•+:DOPh•+ ratios as a function of ionizing energy provides a more rigorous basis for kinetic analysis of the data. The first differential of the HOPh•+:DOPh•+ ratio as a function of photon energy allows a comparison of monoenergetic ions. However, as will be presented below, we believe that a phenomenological picture (as opposed to use of a mechanistic model) leads to a misleading interpretation of the experimental results. Figure 1 depicts the first differential photoionization energy (PIE) curves for undeuterated **1**. Onset of ionization corresponds to an adiabatic ionization energy of IE = 8.08 ± 0.02 eV. The intensity of the molecular ion current (M•+ = *m/z* 136) rises monotonically with the photon energy *hν* until the the extent of fragmentation becomes substantial. The value of the first differential of M•+ is >0 below 10.1 eV. In the domain of this experiment *m/z* 94 is the only fragment ion. The fragment ion current rises monotonically from its onset between 9.8 and 9.9 eV. As a consequence, that curve in Figure 1 is uniformly >0. As can be seen in Figure 1, both curves exhibit crests and troughs at energies >10.5 eV.

In photoionizing molecules with thermal energy ϵ and ionization energy IE, one expects the photoelectrons to be ejected with kinetic energies ranging from zero to $h\nu + \epsilon -$ IE. The fragment ion current at a given value of *hν* thus represents the decomposition of molecular ions having a distribution of internal energies. To a good approximation, however, the first differential of the fragment ion current as a function of *hν* is proportional to the number of fragment ions formed from molecular ions having internal energy equal to $h\nu + \epsilon -$ IE. The *m/z* 94 first differential curve therefore corresponds to a plot of the efficiency of fragmentation as a function of the internal energy of the molecular ion. Deuterated precursors exhibit two fragment ions, HOPh•+ (*m/z* 94) and DOPh•+ (*m/z* 95), and the first differential of the *m/z* 94:*m/z* 95 ratio (corrected for ^{13}C natural abundance) with respect to *hν* represents the relative efficiency of the two competing fragmentations at a given parent ion internal energy.

First differential PIE curves for HOPh•+:DOPh•+ ratios from compounds **1a** and **1b** are reproduced in Figure 2. The two curves are well separated from one another, so it is apparent that mechanism *ii* (complete alkyl hydrogen randomization) cannot be the exclusive pathway at any energy in the domain (for if it were, the result from **1a** would have been the same as from **1b**). The curves in Figure 2 exhibit crests and troughs

(20) Kondrat, R. W.; Morton, T. H. *Org. Mass Spectrom.* **1991**, *26*, 410−415.

(21) Audier, H. E.; Berthomieu, D.; Morton, T. H. *J. Org. Chem.* **1995**, *60*, 7198−7208.
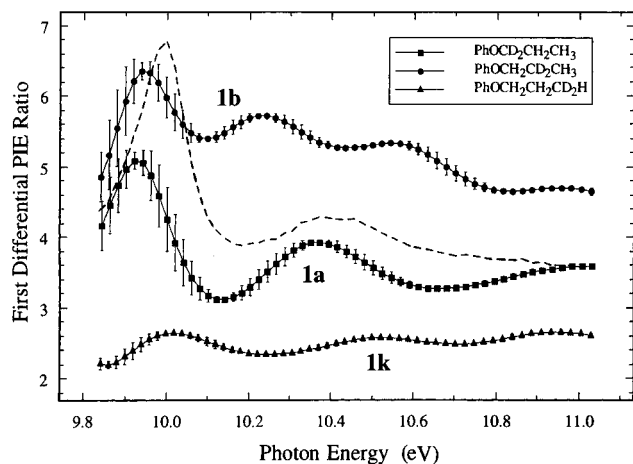
Figure 2. First differential curves of the HOPh$^{•+}$:DOPh$^{•+}$ ratios for the three *gem-n*-propyl-d_2 ethers, **1a**, **1b**, and **1k**. The dashed line shows the value of the ratio R = [first differential ratio from **1b**/first differential ratio from **1d**].$^{1/2}$

Table 1. Mole Fractions of Transfer from Positions $\alpha - \gamma$ (Corresponding to Undeuterated **1**) and Phenomenological Isotope Effects (k_H/k_D) for Perdeuterated Positions
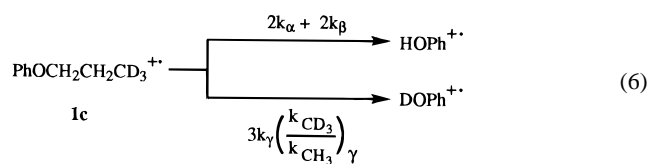
	X_α	X_β	X_γ	$(k_H/k_D)_\alpha$	$(k_H/k_D)_\beta$	$(k_H/k_D)_\gamma$
10.35 eV^a	0.18	0.18	0.65	0.75	1.18	2.25
10.35 eV^b	0.18	0.16	0.65	0.87	1.05	2.33
crests^b	0.15	0.20	0.65	0.68	1.43	2.36
troughs^b	0.20	0.17	0.62	0.82	1.10	2.02

^{a} From ratios of ion currents measured at $h\nu$ = 10.35 eV. ^{b} From first differentials of the ion currents.

<10.5 eV, which do not coincide with any obvious features of the fragment ion curve in Figure 1.
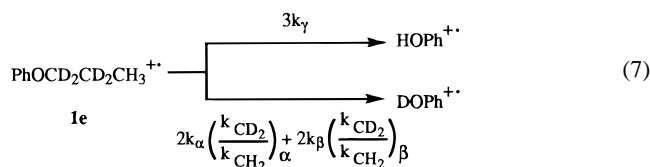
Figure 3 reproduces the first differential PIE curve for the HOPh$^{•+}$:DOPh$^{•+}$ ratio from compound **1c**, while Figure 4 displays the curves for **1d** and the $\alpha,\alpha,\beta,\beta$-$d_4$ compound PhOCD$_2$CD$_2$CH$_3$ (**1e**). The value of ratio R (extracted from the curves for **1b** and **1d**) is plotted as a dashed line in Figure 2. As is apparent, R is >5 at 10 eV but falls to 3.6−4.3 (comparable to the value reported from the MIKES spectrum[11]) in the domain 10.1−11.0 eV. Clearly mechanism *iii* by itself cannot account for the high value of R near 10 eV. A more detailed analysis of the data shows that pathway *v* contributes to varying extents, depending on the deuterium labeling pattern.

Equations 6 and 7 illustrate how phenomenological values of X_α, X_β, and X_γ were estimated from the experimental data by assuming an independent isotope effect for each position of the chain. A set of five schemes (eqs 6 and 7, along with analogous schemes for **1a,b,d**) provides a basis for analyzing ratios from the first differential curves for **1a−e**. Several of these curves exhibit pronounced crests and troughs, which do not necessarily coincide with one another for different deuterated analogues. This is not surprising, since kinetic shifts of different isotopomers need not be identical; hence, one PIE curve may be displaced from another. In substituting experimental ratios for **1a−e** into the five equations with five unknowns, one cannot decide *a priori* whether data points should be selected at crests (or troughs) at energies that are close to one another, or whether

$$(6)$$

data points should all be taken at the same value of $h\nu$. It turns

out that most of the curves have crests at 10.35 eV, and all have troughs within ±0.15 eV of 10.5 eV. Table 1 summarizes the values of $X_\alpha - X_\gamma$ extrapolated for undeuterated **1** (and the corresponding phenomenological isotope effects) calculated at

$$(7)$$

10.35 eV (using either the ratio of ion currents or the first differential at that photon energy), at the crests (using the local maxima in the first derivative curve near 10.25 eV for **1b** and **1d** in place of the ratios at 10.35 eV), and at the troughs near 10.5 eV. The difference among the values thus derived represents an estimate of systematic error. Since X_α is less than the statistical value expected for pure *ii* ($\frac{2}{7}$) it does not seem likely that pathway *iv* (pure α-transfer) plays any significant role.

To dissect the relative contributions of *i*, *ii*, *iii*, and *v*, six more deuterated propyl phenyl ethers were studied: another d_3 analogue, PhOCH$_2$CD$_2$CH$_2$D (**1f**), as well as three d_1 analogues, PhOCH$_2$CH$_2$CH$_2$D (**1g**), PhOCH$_2$CHDCH$_3$ (**1h**), and PhOCHDCH$_2$CH$_3$ (**1i**). In addition two other d_2 analogues were examined, PhOCH$_2$CHDCH$_2$D (**1j**) and PhOCH$_2$CH$_2$CD$_2$H (**1k**). The PIE curve for **1j** (not shown) exhibits a shoulder at 10.35 eV (HOPh$^{•+}$:DOPh$^{•+}$ = 4.35) and a trough at 10.55 eV (HOPh$^{•+}$:DOPh$^{•+}$ = 3.6). Figure 5 reproduces the first differential PIE curves for the d_1 analogues.

Consider the contrast between the curves for **1a** and **1k** in Figure 2. If pathways *i−iii* operated to the same extent for both **1a** and **1k**, their HOPh$^{•+}$:DOPh$^{•+}$ ratios should have been equal. If only pathway *iii* were operating for **1a** and only pathway *ii* were operating for **1k**, the ratio for the former would have been $\frac{5}{2}\frac{4}{2}$ = 1.25 times that of the latter (assuming the same proton transfer isotope effects for *ii* and *iii*). Allowing both *ii* and *iii* to operate for **1a** or **1k** would diminish this ratio of ratios, as would permitting *i* or *iv* (or both) to operate in competition. Since the experimental ratio of ratios is 1.62 at 10.35 eV, pathway *v* must be invoked.

We draw the following distinction between a phenomenological picture and a mechanistic model to interpret these results. A phenomenological picture uses the ten data points to assess the relative contributions of positions α-γ as well as eight independent primary and secondary isotope effects. A mechanistic model assumes a specific set of competing pathways and evaluates isotope effects for appropriate steps. While a phenomenological picture gives an exact, unique solution for the ten equations in ten unknowns, the results in Table 1 imply that at least three-eighths of ionized **1** decomposes via *v*, a conclusion that is hard to accept. Moreover, we cannot assess from a phenomenological picture the proportions of *i−iii* that accompany *v*. To do this requires that we go beyond a phenomenological picture: the data from **1a−j** must instead be fitted to a composite of four pathways. However, the additional constraint imposed by such a mechanistic model means that observed and calculated data points may no longer agree exactly. In examining six different mechanistic models, we report the one that gives the best fit.

One criterion of quality of fit is the agreement between calculated and observed values for **1k**. For this compound the ratio at 10.35 eV, HOPh$^{•+}$:DOPh$^{•+}$ = 2.42, comes close to a trough in the first differential curve. Phenomenological predictions of the value for **1k** range from 1.71 (based on ratios of
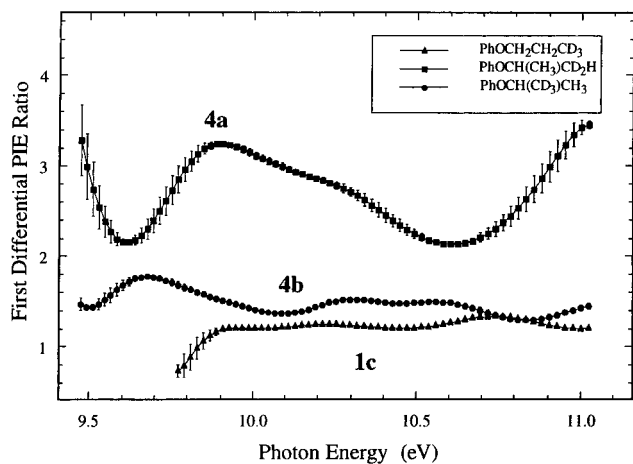
Figure 3. First differential curves of the HOPh$^{\bullet+}$:DOPh$^{\bullet+}$ ratios for methyl-d_3 n-propyl and isopropyl phenyl ethers (**1c** and **4b**) and *gem* isopropyl-d_2 phenyl ether (**4a**).

ion currents at 10.35 eV) and 1.86 (based on troughs near 10.5 eV in the first differential curves), to 2.34 (based on first differentials at 10.35 eV) and 2.36 (based on crests near 10.35 eV in the first differential curves, as compared with a crest value of 2.6 at 10.5 eV). While none of the predictions matches the respective observed value exactly, the result from first differentials at 10.35 eV comes closest. Therefore calculations for mechanistic models were also performed using first differentials at 10.35 eV.

A mechanistic model explicitly weighs the contributions of individual pathways, but i–v are not linearly independent. Because the preponderance of evidence suggests that iv is very minor, it will be neglected, and only the percent contributions of pathways i, ii, iii, and v are considered. The first differential ratios for **1a**–**j** at 10.35 eV can then be used to predict a value for **1k** and also to extract a HOPh$^{\bullet+}$:DOPh$^{\bullet+}$ ratio for each of the individual pathways. The Discussion section compares HOPh$^{\bullet+}$:DOPh$^{\bullet+}$ ratios corresponding to pathway iii by itself with the HOPh$^{\bullet+}$:DOPh$^{\bullet+}$ ratios for the isopropyl-d_2 phenyl ether **4a** and the isopropyl-d_3 ether **4b**. Figure 3 displays the first differential PIE curves for these isopropyl ethers, and the curve for **1c** is seen to be well separated from that for for **4b**. The onset of ionization for **4** corresponds to an adiabatic IE of 7.98 ± 0.02 eV. Given that the isomerization of ionized **1** to ionized **4** is exothermic and that elimination of propene from ionized **4** has a lower barrier than from ionized **1**,[16] it is conceivable that pathway iii operates via the intermediacy of ionized **4**. As shall be discussed below, comparison of **4a** with **1k** and of **4b** with **1c** shows that the n-propyl and isopropyl systems manifest different isotope effects.

Discussion

This experimental investigation has three principal objectives: (1) to assess relative contributions of competing pathways to propene expulsion from nPrOPh$^{\bullet+}$; (2) to gauge isotope effects for eq 3 and compare them with the isotope effect for propene expulsion from iPrOPh$^{\bullet+}$ (ionized **4**); and (3) to provide an explanation for the reported conformational dependence[14] of HOPh$^{\bullet+}$:DOPh$^{\bullet+}$ ratios in supersonic jet/REMPI mass spectra of deuterated **1**.

While some organic reactions proceed specifically via a single mechanism, many others take place via several pathways, all of which operate concurrently to yield the same final product. The present data reveal that expulsion of propene from ionized n-propyl phenyl ether falls into this second category. Our investigation makes use of first differential ionization efficiency

curves to control for the internal energy spread of photoions,[22] so that first-order kinetics may appropriately be applied to extract mechanistic information. The discussion below will focus on photoionization at $h\nu = 10.35$ eV, but the PIE curves reproduced in Figures 1–5 suggest that the conclusions hold true for the entire domain 10–11 eV. This particular value of $h\nu$ is chosen because it corresponds to the point where the first differential PIE curve for the molecular ion manifests its first local minimum in Figure 1. Also, most of the first differential HOPh$^{\bullet+}$:DOPh$^{\bullet+}$ ratios exhibit local maxima at this energy, and here the results for ratios of ion currents do not differ greatly from the results from the first differential curves. From the measured IE of n-propyl phenyl ether (8.08 eV), the internal energy of ions at $h\nu = 10.35$ eV in the first differential curve is 2.27 ± .03 eV, which is 10.35 − 8.08 − 1.47 = 0.80 ± 0.05 eV above the energy barrier for propene expulsion.[16]

Relative Contributions of Competing Pathways. HOPh$^{\bullet+}$:DOPh$^{\bullet+}$ ratios for the ten deuterated analogues **1a**–**j** were fitted using seven independent isotope effects applied to the competition among pathways i, ii, iii, and v. While a unique solution is easily obtained for a phenomenological analysis of these ten data points, a perfect fit is not easily achieved when a specific mechanistic model is imposed. Because many more isotope effects can be imagined than there are data, it has been necessary to combine several of them. In the best fit, the primary isotope effect for D-shift from a β-CHD in pathway iii (relative to H-shift from a CH$_2$) was set equal to the primary isotope effects for pathways i and v. These three isotope effects are taken all to have the same value, $k_H/k_D = x$. Similarly, the primary isotope effects for D$^+$-transfer from deuterated propyl ions within complexes were taken to be the same, regardless of whether the ion scrambles (pathway ii) or not (pathway iii). These isotope effects have the value $k_H/k_D = y$. Secondary isotope effects were neglected for all of these reactions. The only secondary isotope effects explicitly considered were those that affect the first step of pathway iii: the α-, β-, and γ-position secondary isotope effects (treated independently of one another) on the hydride shift that isomerizes n-propyl to isopropyl cation (e.g., the H-shift from β-CHD relative to β-CH$_2$, whose value is represented as $k_H/k_D = z$). A separate isotope effect for D-shift from β-CD$_2$ was used. Finally, the isotope effect on the competition between ii and iii was explicitly considered and found to be large. This last isotope effect was taken to be multiplicative (i.e., the effect for n deuteria was assumed equal to the effect for one deuterium raised to the nth power), as were the α- and γ-position secondary isotope effects on hydride transfer.

Isotopic substitution is found to affect the branching among competing pathways. The sum of the contributions of i and v is small (≤5.5%) except where position α is deuterated (**1a**, **1d**, **1e**, and **1i**). In these latter cases the contribution of v is greater than that of i. Compound **1d** is the only instance where the contribution of i exceeds 4%. According to the mechanistic model undeuterated **1** should give only small proportions of i and v: extrapolation predicts X$_\alpha$ = 0.29, X$_\beta$ = 0.26, and X$_\gamma$ = 0.45, considerably different from the contributions predicted phenomenologically in Table 1.

The discrepancy between the phenomenological picture and the mechanistic model signals a defect in the approximations underlying the former. Were i, iv, and v the only pathways in operation, the two interpretations would coincide. It would then have been reasonable to suppose (as in eq 7) the isotope effects

(22) Hurzeler, H.; Inghram, M. G.; Morrison, J. D. *J. Chem. Phys.* **1958**, *28*, 76–82.
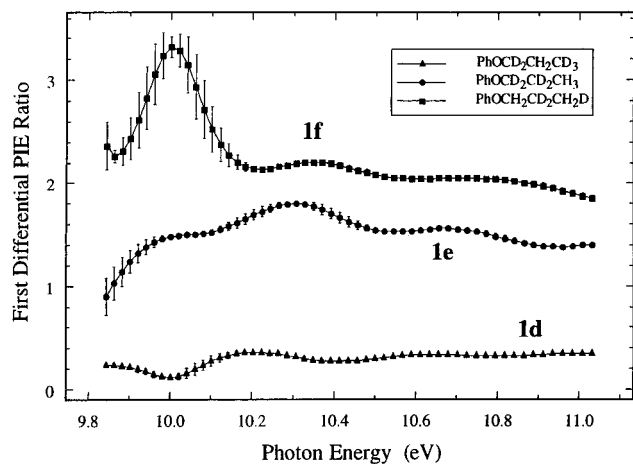
Figure 4. First differential curves of the HOPh$^{\bullet+}$:DOPh$^{\bullet+}$ ratios for *n*-propyl phenyl ethers having ≥ 3 deuteria with isotopic substitution on two carbons (**1d**–**f**).

Figure 5. First differential curves of the HOPh$^{\bullet+}$:DOPh$^{\bullet+}$ ratios for the three *n*-propyl-d_1 phenyl ethers, **1g**–**i**.
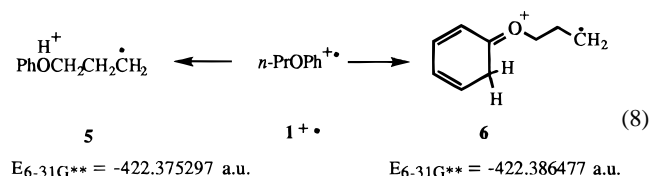
Table 2. Best Fit between Model (Parameters Extracted from Data for **1a**–**j**) and Experiment, with Calculated Percentages of Competing Pathways *i*, *ii*, *iii*, and *v* at 10.35 eV

	HOPh$^{\bullet+}$:DOPh$^{\bullet+}$			percent each pathway (calcd from **1a**–**j**)^b			
	obsd^a	obsd^b	calcd^b	i	ii	iii	v
1-d_0	∞	∞	∞	0.5^c	81.2^c	16.5^c	1.8^c
1a	3.52	3.85	3.74	3.6	68.6	13.9	14.0
1b	5.46	5.40	5.35	0.2	17.3	78.9	3.5
1c	1.23	1.24	1.23	1.0	6.6	91.1	1.2
1d	0.34	0.33	0.33	8.0	5.7	77.9	8.6
1e	1.68	1.78	1.77	2.0	13.2	60.4	24.3
1f	2.52	2.41	2.40	0.2	5.0	92.4	2.4
1g	5.95	6.93	6.75	0.9	52.8	43.5	2.8
1h	12.8	11.3	11.1	0.7	61.2	33.9	4.2
1i	7.85	7.73	7.60	1.4	77.6	15.7	5.3
1j	5.45	4.37	4.33	1.0	29.1	65.5	4.5
1k	2.42	2.42	2.56^c	1.2^c	22.2^c	74.3^c	2.3^c
1-d_7			0	1.1^c	0.3^c	94.4^c	4.2^c

^{a} Ratios of HOPh$^{\bullet+}$ to DOPh$^{\bullet+}$ion currents measured at $h\nu = 10.35$ eV. ^{b} From first differentials of the ion currents. ^{c} Predicted from parameters based on **1a**–**j**.

for positions α and β to be independent of one another. The mechanistic model does not make such an assumption. In the phenomenological picture (given a normal isotope effect) β-deuteration ought to choke off β-transfer, thereby increasing the mole fractions of α- and γ-transfer. By contrast, the mechanistic model concludes that a β-CD$_2$ suppresses *i* (augmenting *v*) but at the same time enhances *iii* at the expense of *ii*. Since the statistical weight of position α in *iii* is $\frac{1}{3}$ (which is

greater than in *ii*), the net effect is opposite to what the phenomenological model would predict. For example, from Table 2 and $y = 1.21$ we determine that **1a** transfers 20% from α and 21% from β, while **1b** transfers 25% from α and 15% from β. Nevertheless, **1e** transfers 19% from α and 16% from β, exhibiting an attenuation of α-transfer as a consequence of β-deuteration. In conclusion, the assumptions underlying the phenomenological picture do not coincide with conclusions drawn from the mechanistic model. Between the two, the mechanistic model is to be preferred.

$$E_{\text{6-31G**}} = -422.375297 \text{ a.u.} \qquad E_{\text{6-31G**}} = -422.386477 \text{ a.u.} \tag{8}$$

Regardless of how the experimental data are interpreted, site-specific γ-transfer (pathway *v*) operates to a measurable extent. UHF calculations set the γ-distonic ion **5** 164 kJ mol^{-1} (including a 2 kJ mol^{-1} difference in zero point energy) above *n*PrOPh$^{\bullet+}$, more than 20 kJ mol^{-1} above the experimental barrier height. Since previously published experiments[5,7] have already shown that the role of pathway *v* increases as internal energy decreases (a result qualitatively in agreement with the data presented here), ab initio calculations would appear to militate against the intermediacy of **5**. The tautomeric γ-distonic ion **6** is 29 kJ mol^{-1} lower than **5**. For **6** to be consistent with the reported overall barrier height, the activation energy for the intramolecular hydrogen atom abstraction **1**$^{\bullet+} \rightarrow$ **6** would have to be <7 kJ mol^{-1}. Although we have made no effort to compute this transition state, it seems unlikely that the barrier to hydrogen transfer could be this low. Moreover, for **6** to serve an an intermediate it would have to undergo additional rearrangement to give HOPh$^{\bullet+}$, the structure that has been shown to be the exclusive product of propene elimination from **1**$^{\bullet+}$.[16]

Ab initio calculations place ion−neutral complex **2** slightly below the experimental barrier for eq 1.[16] We have previously reported **2** as a local minimum (based on UHF normal modes at 3-21G), but we find that the geometry achieved by conventional optimization procedures at 6-31G** exhibits two negative force constants and is predicted to collapse without a barrier to **4**$^{\bullet+}$. Despite that computational prediction, Figure 3 provides experimental evidence that collapse does not compete effectively against proton transfer (the second step of eq 3). The next section provides the rationale behind this interpretation.

Isotope Effects for *n*PrOPh$^{\bullet+}$ Compared to *i*PrOPh$^{\bullet+}$. The most important derived isotope effects in this study are those that act on pathway *iii*: the preference for H- versus D-shift from the β-position (the first step of eq 3, for which $x/z = 6.5 \pm 0.9$) and the normal isotope effect that we assign to the second step of eq 3 ($y = 1.21 \pm 0.03$). These have appropriate magnitudes for a hydride shift and a proton transfer, respectively. The remaining isotope effects are best expressed in terms of the relative proportions of competing pathways summarized in Table 2. Extrapolation to a perdeuterated propyl side chain predicts nearly complete suppression of *ii*.
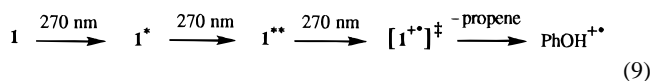
Now consider the operation of pathway *iii*. Strictly speaking, this pathway represents isomerization of the *n*-propyl side chain to an isopropyl without any further transposition of hydrogen. Equation 3 portrays what we infer takes place. Alternatively, rearrangement might have occurred via collapse of an [*i*Pr$^+$ PhO$^{\bullet}$] ion−neutral complex to **4**$^{\bullet+}$, followed by propene expulsion. The value of $y(k_H/k_D$ for proton transfer from propyl to phenoxy) is of particular relevance in assessing whether **4**$^{\bullet+}$

intervenes. From previous work ionized **4** is known to expel propene more rapidly than does ionized **1** with the same internal energy.[16] While it is thus plausible for pathway *iii* to proceed via the sequence $1^{\bullet+} \rightarrow 4^{\bullet+} \rightarrow$ propene + PhOH$^{\bullet+}$, a comparison of isotope effects demonstrates that ionized **1** does not decompose in this fashion.

If pathway *iii* did happen to pass through *i*PrOPh$^{\bullet+}$, **1k** would isomerize to **4a** and **1c** would isomerize to **4b**. However, the HOPh$^{\bullet+}$:DOPh$^{\bullet+}$ ratios for **4a** and **4b** at 10.35 eV, 2.68 ± 0.06 and 1.53 ± 0.01, are larger than for **1k** and **1c**. Correcting the **1k** and **1c** results for contributions from *i*, *ii*, and *v* does not bring their HOPh$^{\bullet+}$:DOPh$^{\bullet+}$ ratios into line with those from **4a** and **4b**. Since the heat of formation of $4^{\bullet+}$ is 0.2 eV less than that of $1^{\bullet+}$, it may be more appropriate to compare the 10.35 eV ratios from **1k** and **1c** with values from **4a** and **4b** at lower energies. The ratio for **4a** is HOPh$^{\bullet+}$:DOPh$^{\bullet+}$ = 3.03 at 10.1 eV, which declines monotonically with increasing energy over the next 0.5 eV, as Figure 3 depicts. Below 10.4 eV, the ratio from **4a** remains significantly higher than the ratio from **1k**. For **4b** the ratio has its minimum value at 10.1 eV, HOPh$^{\bullet+}$: DOPh$^{\bullet+}$ = 1.38, which is larger than the ratio from **1c** over the domain from onset up to 10.75 eV (as can be seen from Figure 3).

Since $4^{\bullet+}$ is known not to transpose hydrogens prior to propene expulsion,[16] isotope effects are calculated in a straightforward fashion for the isopropyl system. Competition between CH_3 and CD_3 is simply the HOPh$^{\bullet+}$:DOPh$^{\bullet+}$ ratio from **4b** and ranges from $k_H/k_D = 1.38{-}1.62$ in the domain 9.8–10.4 eV. For the competition between CH_3 and CD_2H the average k_H/k_D equals half the ratio from **4a** and has a value of 1.35 ± 0.08 in that domain. For isopropyl phenyl ether it is apparent that k_H/k_D for H- versus D-transfer from a CD_2H must differ slightly from competition between a CH_3 and a CD_3. Nevertheless, the contrast to the *n*-propyl case, $y = 1.21$, is significant. Hence we conclude that, although $4^{\bullet+}$ would have been a kinetically competent intermediate, pathway *iii* proceeds as shown in eq 3 and not via collapse of complex **2** to a covalently bonded ion. Neither does $4^{\bullet+}$ pass through complex **2** when it expels propene, in agreement with previous work.[16] *n*-Propyl and isopropyl parent ions eliminate via separate routes.

Conformational Dependence of HOPh$^{\bullet+}$:DOPh$^{\bullet+}$ Ratios. Supersonic jet/REMPI spectroscopy allows examination of the mass spectra of individual conformational isomers of neutral precursors. In such experiments, a cold gaseous molecule is promoted to its first excited state (a resonant transition) and then ionized by absorption of a second photon. When REMPI is performed using a (0,0)-transition as the resonant absorption, the electronically excited neutral is vibrationally cold. If the excited state geometry does not differ greatly from that of the ground state, then the conformation will not change in the short time required for the subsequent ionization.
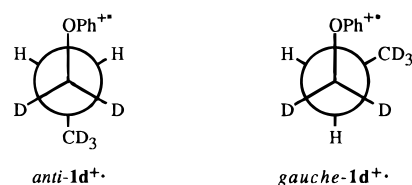
$$1 \xrightarrow{270 \text{ nm}} 1^* \xrightarrow{270 \text{ nm}} 1^{**} \xrightarrow{270 \text{ nm}} [1^{\bullet+}]^{\ddagger} \xrightarrow{-\text{propene}} \text{PhOH}^{\bullet+}$$
(9)

The barrier to propene expulsion from $1^{\bullet+}$ is so high[16] that three photons have to be absorbed at the (0,0) transition wavelength (near 270 nm) in order to observe any fragmentation, as eq 9 summarizes. The excitation spectrum of **1** contains peaks from three separate conformers, in proportions that probably reflect their relative abundances at room temperature.[23] REMPI mass spectra of **1d** (using 10^{-8} s laser pulses tuned to (0,0)-transitions) exhibit HOPh$^{\bullet+}$:DOPh$^{\bullet+}$ ratios that depend upon conformation.[14] The variation among rotamers for **1b** is not statistically significant. Table 2 provides an explanation

for the more robust conformational effect in **1d**: pathways *i* and *v* together constitute one-sixth of the fragmentation for **1d**, but less than 4% of the fragmentation for **1b**. The competition between formation of [propyl ion phenoxy radical] complexes and these other pathways leads to a conformational sensitivity of the mass spectra for **1d** that is more pronounced than for **1b**.

$$\begin{array}{cc} \text{CH}_3\text{CHCCHD}_2 & \text{CH}_3\text{CHCCD}_3 \\ | & | \\ \text{OPh} & \text{OPh} \\ \mathbf{4a} & \mathbf{4b} \end{array}$$

How might conformation affect this competition? Two general hypotheses must be weighed. The first stipulates that different conformers yield different distributions of excited $1^{\bullet+}$ upon multiphoton ionization. If UV photoelectron spectra of homologues of **1** serve as a guide,[6] many different doublet states are accessible <13.8 eV (the energy of three 270 nm photons) above the ground state neutral. Energy deposition by three-photon ionization could well depend upon conformation, particularly since the power dependence of the phenol$^{\bullet+}$ yield indicates that eq 9 (where 1^{**} stands for a superexcited neutral and $[1^{\bullet+}]^{\ddagger}$ a vibrationally excited doublet in its lowest electronic state) functions in parallel with the better-known ladder-switching mechanism.[14] If the conformation effect is simply a matter of internal energy content, this hypothesis suggests that other alkyl phenyl ethers should also manifest conformation-dependent mass spectra, provided they have fragmentation patterns at least as sensitive to internal energy as that of **1d**.

anti-1d$^{+\bullet}$ *gauche*-1d$^{+\bullet}$

$E_{6\text{-}31G^{**}} = -422.438598$ a.u. $E_{6\text{-}31G^{**}} = -422.438428$ a.u.

The second hypothesis presupposes that the rotameric equilibrium of ionized **1** is affected by the structure of the neutral precursor. It is hard to imagine that $[1^{\bullet+}]^{\ddagger}$ decomposes before complete rotameric equilibration is achieved. The SCF electronic energy barrier to conversion of *anti*-$1^{\bullet+}$ to *gauche*-$1^{\bullet+}$ (which have the same stability) is slightly less than we calculate for the conversion of neutral, planar *anti*-**1** to the more stable neutral *gauche*-**1** (15 kJ mol^{-1} for the former versus 16 kJ mol^{-1} for the latter). Assuming rapid preequilibrium of *anti*-**1d**$^{\bullet+}$ with *gauche*-**1d**$^{\bullet+}$, memory of the conformation of the neutral precursor should govern the relative proportions only for pathways that require the propyl group to rearrange simultaneously with C–O bond cleavage. The coplanar C-methyl and O-methylene bonds in the *anti* rotamer are better set up for eq 5 than in the *gauche*. Suppose a neutral precursor in the *anti* conformation leads to a greater fraction of reactive *anti* ions. This would predict more net transfer from the γ-position and, hence, a lower HOPh$^{\bullet+}$:DOPh$^{\bullet+}$ ratio for *anti*-**1d** and a higher ratio for *anti*-**1b** (relative to their *gauche* rotamers), as has been reported experimentally.[14]

$$\text{ROPh}^{\bullet+} \rightarrow [\text{R}^+ \quad \text{PhO}^{\bullet}] \rightarrow [\text{R}'^+ \quad \text{PhO}^{\bullet}] \rightarrow \text{HOPh}^{\bullet+} \quad (10)$$

Either explanation predicts that **1e** ought to manifest an even more pronounced dependence of its HOPh$^{\bullet+}$:DOPh$^{\bullet+}$ ratio than

(23) Ruoff, R. S.; Klots, T. D.; Emilsson, T.; Gutowsky, H. S. *J. Chem. Phys.* **1990**, *93*, 3142–3150.

(24) Winstein, S.; Holness, N. J. *J. Am. Chem. Soc.* **1955**, *77*, 5562–5578.

has been observed for **1d**. On the other hand, it also implies heterolyses that produce stable ions (even if they fall into shallow potential energy minima) will not show conformation-dependent mass spectra. Equation 10 exemplifies a general case, where R^+ stands for a cation with the same connectivity as its neutral precursor, while R'^+ symbolizes a rearranged cation. Here we speculate that R^+ should endure long enough to lose all dependence upon the geometry of its antecedents. As noted above, $\mathbf{1}^{\bullet+}$ does not fall into the category of reactions represented by eq 10. Since the primary *n*-propyl cation has no discrete existence, $nPrOPh^{\bullet+}$ passes directly to a complex containing a rearranged cation. However, other ionized alkyl phenyl ethers may well decompose as eq 10 represents.

The present results provide further illustration of the analogy between gas phase decompositions of ionized *n*-alkyl phenyl ethers and solvolysis chemistry. More than 40 years ago, Winstein and Holness noted that functionalized cyclohexanes undergo S_N1 reactions as equilibrating mixtures of conformational isomers, which they were able to lock into place by means of *tert*-butyl substituents.[24] In an analogous fashion, ionization of conformationally frozen neutrals may permit a glimpse of rotameric effects on bond heterolyses in acyclic systems. If ions produced by REMPI do exhibit memory effects as described by the processes outlined above, then the presence or absence of conformational dependence might serve as a tool for assessing whether carbocations rearrange in concert with the bond heterolyses that form them.

Conclusions

The experiments described above lead to the following findings:

(1) Using a mechanistic model we extract the relative proportions of pathways *i*, *ii*, *iii*, and *v* in unimolecular dissociations of ionized *n*-propyl phenyl ether (**1**) and its deuterated analogues. Pathway *iii*, which passes through [*i*Pr$^+$ PhO$^{\bullet}$] ion−neutral complexes (**2**), predominates for ions with internal energies 0.8 eV above the dissociation barrier.

(2) Deuterium substitution significantly affects the proportions of competing pathways. This phenomenon has been noted in other gas phase reactions, to which the term "metabolic switching" has been applied by analogy to isotope effects in enzyme-catalyzed reactions.[25] As a consequence, a purely phenomenological picture leads to an incorrect interpretation of the data for **1**, predicting an implausibly high contribution from site-specific γ-transfer (*v*). The contribution of this pathway from mechanistic analysis, while not zero, is more consistent with the extent of cyclopropane formation reported from solution studies of nascent primary alkyl cations.[2]

(3) Isotope effects for ionized **1c** and **1k** are significantly lower than for the isopropyl isomers **4a** and **4b** at the same internal energy. Consequently isomerization of $nPrOPh^{\bullet+}$ to $iPrOPh^{\bullet+}$ does not occur (at least, not as the dominant mechanism). Ionized **1** produces **2**, which then expels propene via proton transfer from the isopropyl cation to the phenoxy radical.

(4) α-Deuteration of **1** leads to increased participation of pathway *v*, which we believe passes through ion−neutral complex **3**. Competition between this pathway and formation of [propyl ion PhO$^{\bullet}$] complexes is sensitive to neutral precursor conformation.

The mechanistic analysis described here considers branching among four pathways (perhaps somewhat artificially). It is plausible that some of these pathways should be combined. For instance, ion−neutral complex **3** might be the initially formed intermediate for both pathways *iii* and *v*, with transposition of hydrogen simply competing with the proton transfer shown in eq 5. Such hypotheses lead to predictions, for which experimental tests are presently being devised.

Supporting Information Available: RHF and UHF geometries at 6-31G** (11 pages). See any current masthead page for ordering and Internet access instructions.

JA9607594

(25) (a) Prüsse, T.; Fiedler, A.; Schwarz, H. *Helv. Chim. Acta* **1991**, *74*, 1127−1134. (b) Seemeyer, K.; Prüsse, T.; Schwarz, H. *Helv. Chim. Acta* **1993**, *76*, 1632−1635. (c) Schalley, C. A.; Schröder, D.; Schwarz, H. *J. Am. Chem. Soc.* **1994**, *116*, 11089−11097. (d) Raabe, N.; Karrass, S.; Schwarz, H. *Chem. Ber.* **1995**, *128*, 649−650. (e) Schalley, C. A.; Schröder, D.; Schwarz, H. *Int. J. Mass Spectrom. Ion Proc.* **1996**, *153*, 173−199.